

Reactive Intermediates in the Photodecarbonylation of the Cyclopentadienyl and Indenyl Complexes $\text{CpFe}(\text{CO})_2(\text{C}(\text{O})\text{CH}_3)$ and $\text{IndFe}(\text{CO})_2(\text{C}(\text{O})\text{CH}_3)$ ($\text{Cp} = \eta^5\text{-C}_5\text{H}_5$; $\text{Ind} = \eta^5\text{-C}_9\text{H}_7$)

Karen L. McFarlane,^{1,†} Brian Lee,[†] Wenfu Fu,[‡] Rudi van Eldik,[‡] and Peter C. Ford^{*,†}

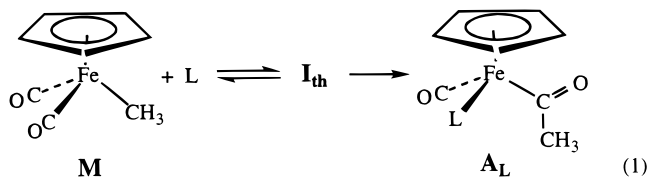
Department of Chemistry, University of California, Santa Barbara, California 93106, and Institute for Inorganic Chemistry, University of Erlangen-Nürnberg, 91058 Erlangen, Germany

Received October 28, 1997

Time-resolved infrared and time-resolved optical spectroscopy have been used to probe further into the spectra and dynamics of reactive intermediates **I** and **I_{ind}** generated by flash photodecarbonylation of the respective acetyl complexes $\text{CpFe}(\text{CO})_2(\text{C}(\text{O})\text{CH}_3)$ (**A**) and $\text{IndFe}(\text{CO})_2(\text{C}(\text{O})\text{CH}_3)$ (**A_{ind}**) ($\text{Cp} = \eta^5\text{-C}_5\text{H}_5$; $\text{Ind} = \eta^5\text{-C}_9\text{H}_7$). The competitive reaction dynamics of CH_3 migration to the metal, trapping by CO, and trapping by other ligands such as $\text{P}(\text{OCH}_3)_3$ were determined for these intermediates in various solvents. Hydrostatic pressure effects on the competitive photoreaction pathways for both **A** and **A_{ind}** in hexane solutions were also examined, and it was found that the photosubstitution pathway has a significantly more negative activation volume than does the photoinduced methyl migration (although a less negative value was found than that previously reported from these laboratories). The indenyl intermediate **I_{ind}** is about 5-fold more reactive toward methyl migration and toward trapping by various ligands than is the cyclopentadienyl analogue **I**, but these differences appear to be too small to support a ring-slip mechanism for either type of reaction. The overall picture points to solvento species, e.g., $\text{CpFe}(\text{CO})(\text{Sol})(\text{C}(\text{O})\text{CH}_3)$, as the most likely form of the intermediates for all solvent systems studied at ambient temperature, with the possible exception of the solutions in perfluoro(methylcyclohexane). The possible relevance of these species to mechanisms for migratory insertion of CO into the metal–alkyl bonds of the methyl complexes $\text{CpFe}(\text{CO})_2\text{CH}_3$ (**M**) and $\text{IndFe}(\text{CO})_2\text{CH}_3$ (**M_{ind}**) is discussed.

Introduction

The “insertion” of CO into metal alkyl bonds is the key carbon–carbon bond-formation step in various catalytic schemes for carbon monoxide activation, such as methanol carbonylation to acetic acid and alkene hydroformylation.² The mechanism has been extensively studied for prototypes such as $\text{Mn}(\text{CO})_5\text{R}$ and $\text{CpFe}(\text{CO})_2\text{R}$ ($\text{R} = \text{alkyl}$, $\text{Cp} = \eta^5\text{-C}_5\text{H}_5$), e.g.,



using thermal chemical techniques;^{3,4} however, such methods face difficulties in elucidating the structures and reactivities of reactive intermediates formed in low steady-state concentrations.⁵ In this context, recent

studies at Santa Barbara have focused on the application of flash photolysis methodologies to generate possibly relevant intermediates from suitable precursors and to interrogate these short-lived species using time-resolved optical (TRO) and time-resolved infrared (TRIR) spectral methods.^{6–10} The TRIR technique is especially

(2) (a) Parshall, G. W.; Ittel, S. D. *Homogeneous Catalysis*; John Wiley & Sons: New York, 1992. (b) *Homogeneous Transition Metal Catalyzed Reactions*; Moser, W. R.; Slocum, D. W., Eds.; Advances in Chemistry Series 230; American Chemical Society: Washington, DC, 1992. (c) Klingler, R. J.; Rathke, J. W. *Prog. Inorg. Chem.* **1991**, *39*, 1311. (d) Henrici-Olivé, G.; Olivé, S. *Catalyzed Hydrogenation of Carbon Monoxide*; Springer-Verlag: Berlin, 1984.

(3) (a) Mawby, R. J.; Basolo, F.; Pearson, R. G. *J. Am. Chem. Soc.* **1964**, *86*, 3994–3999. (b) Wojcicki, A. *Adv. Organomet. Chem.* **1973**, *11*, 87–145. (c) Calderazzo, F. *Angew. Chem., Int. Ed. Engl.* **1977**, *16*, 299–311. (d) Flood, T. C.; Jensen, J. E.; Statler, J. A. *J. Am. Chem. Soc.* **1981**, *103*, 4410. (e) Webb, S.; Giandomenico, C.; Halpern, J. *J. Am. Chem. Soc.* **1986**, *108*, 345–347.

(4) (a) Butler, I. S.; Basolo, F.; Pearson, R. G. *Inorg. Chem.* **1967**, *6*, 2074–2079. (b) Green, M.; Westlake, D. J. *J. Chem. Soc. A* **1971**, 367–371. (c) Cotton, J. D.; Crisp, G. T.; Latifah, L. *Inorg. Chim. Acta* **1981**, *47*, 171–176. (d) Nicholas, K.; Raghu, S.; Rosenblum, M. *J. Organomet. Chem.* **1974**, *78*, 133–137.

(5) Collman, J. P.; Hegedus, L. S.; Norton, J. R.; Finke, R. G. *Principles and Applications of Organotransition Metal Chemistry*; University Science Books: Mill Valley, CA, 1987; Chapter 6.

(6) Belt, S. T.; Ryba, D. W.; Ford, P. C. *J. Am. Chem. Soc.* **1991**, *113*, 9524–9528.

(7) Boese, W. T.; Lee, B.; Ryba, D. W.; Belt, S. T.; Ford, P. C. *Organometallics* **1993**, *12*, 4739–4741.

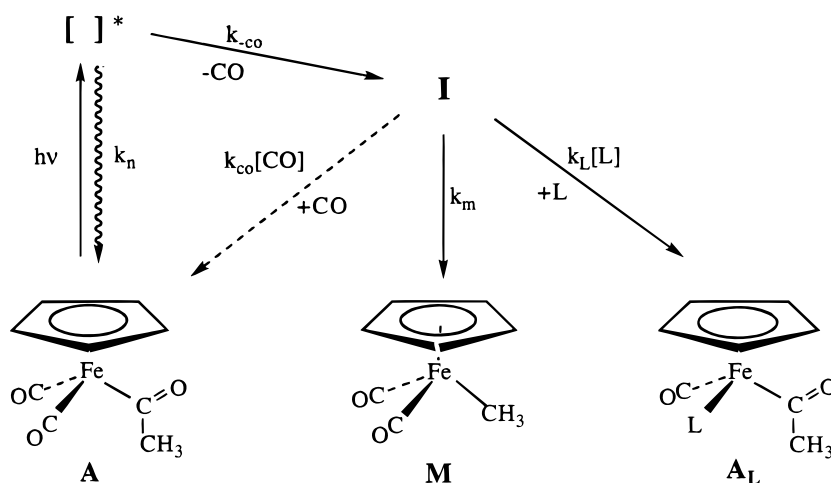
(8) Boese, W. T.; Ford, P. C. *J. Am. Chem. Soc.* **1995**, *117*, 8381–8391.

[†] University of California.

[‡] University of Erlangen-Nürnberg.

(1) Taken in part from the Ph.D. Dissertation of K. L. McFarlane, University of California, Santa Barbara, 1996. Reported in part at the 209th National Meeting of the American Chemical Society, Anaheim, CA, April 1995; American Chemical Society: Washington, DC, 1995; INORG 263.

Scheme 1

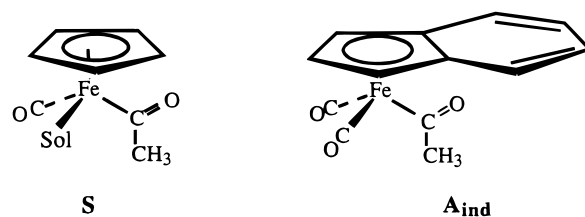


useful since ν_{CO} bands often allow resolution of individual species and serve as probes of electronic properties at the metal center.¹¹

For example, if I_{th} resulted from unimolecular CH_3 migration to coordinated CO, it would have the formulation $\text{CpFe}(\text{CO})(\text{C}(\text{O})\text{CH}_3)$. In a previous study,⁶ species of this composition were generated by the flash photolysis of the acetyl complex $\text{CpFe}(\text{CO})_2(\text{C}(\text{O})\text{CH}_3)$ (**A**) and interrogated by TRO and TRIR techniques. The spectroscopic and kinetics properties were interpreted in terms of the reactions illustrated by Scheme 1. These data provided convincing evidence that the intermediate **I** generated photochemically is the solvento species $\text{CpFe}(\text{CO})(\text{Sol})(\text{C}(\text{O})\text{CH}_3)$ (**S**) in THF and acetonitrile. Its nature in less donating media remained ambiguous; structures with the empty coordination site stabilized by an η^2 -acyl group or via an agostic interaction with CH_3 were considered possible options. The studies presented here probe a wider range of solvents and examine the ligand substitution pathway of **I** in greater detail.

Also presented is the redetermination and reevaluation of hydrostatic pressure effects on the k_L and k_m pathways indicated in Scheme 1. In an earlier study in these laboratories,¹⁰ a very large difference between ΔV_L^\ddagger and ΔV_m^\ddagger suggested possible involvement of an η^3 -Cp species (i.e., a "ring-slip" mechanism) in the ligand substitution pathway. This mechanism is probed here by using TRIR spectroscopy to examine the kinetics of the intermediates generated by flash photolysis of the indenyl complex $(\text{Ind})\text{Fe}(\text{CO})_2(\text{C}(\text{O})\text{CH}_3)$ (**A_{ind}**) (Ind = η^5 -C₉H₇) as well as high-pressure continuous photolysis techniques to measure activation volumes. In addition, the pressure studies of the Cp analogue **A** were repeated using a much more definitive FTIR technique for determining the relative concentrations and products. Supporting experiments include FTIR detection of pho-

togenerated intermediates in low-temperature solutions and continuous wave photolysis.



Experimental Section

Materials. Acetonitrile (Aldrich) was stirred over CaH_2 and then distilled from P_2O_5 . Cyclohexane (spectrophotometric grade, B & J Brand, Baxter) and dichloromethane (Fisher) were distilled from CaH_2 under dinitrogen. Dichloroethane (Fisher) was distilled from P_2O_5 under N_2 . Heptane (spectrophotometric grade, Fluka) was distilled from sodium under argon. Methylcyclohexane (MCH) (Aldrich) was treated to remove alkenes¹² and distilled from sodium metal. 2-Methyltetrahydrofuran (MeTHF), 2,5-dimethyltetrahydrofuran (Me₂THF), and 2,2,5,5-tetramethyltetrahydrofuran (Me₄THF) (Aldrich) were distilled from sodium under argon after predrying over CaH_2 . Perfluoromethylcyclohexane (PFMC) (technical grade, Aldrich) was treated to remove hydrocarbons¹³ and then distilled from P_2O_5 under argon. THF (Aldrich) was distilled from sodium benzophenone ketyl solution under N_2 . Trimethyl phosphite (Aldrich) was vacuum distilled after stirring with sodium and was stored in the dark under dinitrogen. Triphenylphosphine (Aldrich) was recrystallized from ethanol. All gases were passed through an Alltech Associates Oxy-trap and a 4 Å molecular sieves/Drierite column before use. Various CO/argon mixtures were purchased from Liquid Carbonics.

$\text{CpFe}(\text{CO})_2(\text{C}(\text{O})\text{CH}_3)$, $(\text{Ind})\text{Fe}(\text{CO})_2$, and $(\text{Ind})\text{Fe}(\text{CO})_2(\text{C}(\text{O})\text{CH}_3)$ were synthesized following published procedures¹⁴ and purified by column chromatography. The substituted acyl complex $\text{CpFe}(\text{CO})(\text{P}(\text{OCH}_3)_3)(\text{C}(\text{O})\text{CH}_3)$ was prepared as follows: A THF solution of $\text{CpFe}(\text{CO})_2\text{CH}_3$ (500 mg, 0.0026 mol) and $\text{P}(\text{OCH}_3)_3$ (0.46 mL, 0.0039 mol) was prepared in the inert-atmosphere box and stirred overnight at 50 °C. After removal

(9) Boese, W. T.; McFarlane, K. L.; Lee, B.; Rabor, J. G.; Ford, P. C. *Coord. Chem. Rev.* **1997**, *159*, 135–151.

(10) Ryba, D. W.; van Eldik, R.; Ford, P. C. *Organometallics* **1993**, *12*, 104–107.

(11) Applications of TRIR techniques have been the subject of several recent reviews. (a) Ford, P. C.; Bridgewater, J. S.; Lee, B. *Photochem. Photobiol.* **1997**, *65*, 57–64. (b) George, M. W.; Poliakoff, M.; Turner, J. J. *Analyst* **1994**, *119*, 551–560. (c) Schoonover, J. R.; Strouse, G. F.; Omberg, K. M.; Dyer, R. B. *Comm. Inorg. Chem.* **1996**, *18*, 165–188.

(12) Concentrated sulfuric acid (140 mL) was stirred with 700 mL of methylcyclohexane for 4 days at room temperature. The orange-brown aqueous layer was removed, and the solvent was washed with deionized water and aqueous sodium carbonate.

(13) Perrin, D. D.; Armarego, W. L. F.; Perrin, D. R. *Purification of Laboratory Chemicals*; Pergamon Press: Oxford, U. K., 1980; p 251.

(14) (a) *Organometallic Syntheses*; Eisch, J. J.; King, R. B., Eds.; Academic Press: London, 1965; Vol. 1, pp 151–152. (b) Jones, D. J.; Mawby, R. J. *Inorg. Chim. Acta* **1972**, *6*, 157.

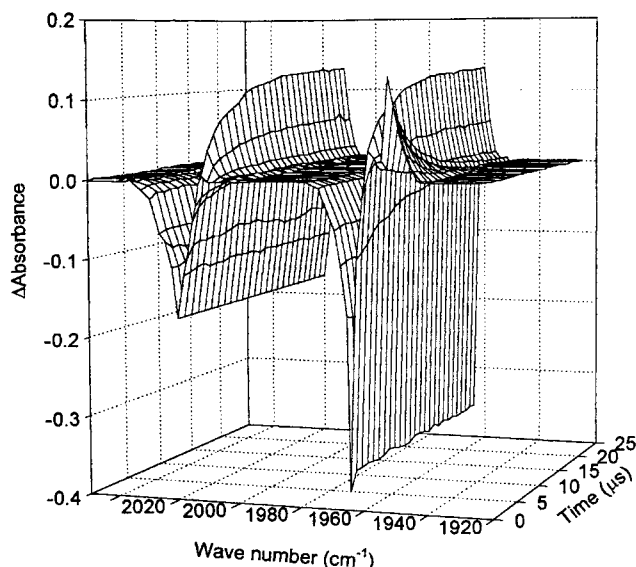


Figure 1. Example of a three-dimensional stack plot of the TRIR spectra illustrating absorbance changes following 308 nm laser flash photolysis of a cyclohexane solution of $\text{CpFe}(\text{CO})_2(\text{C}(\text{O})\text{CD}_3)$ (\mathbf{A}_{43}) under argon at 296 K.

of the solvent, the brown waxy solid was loaded onto a silica-gel column. Unreacted $\text{CpFe}(\text{CO})_2\text{CH}_3$ eluted with a 1:1 (v/v) mixture of hexanes and dichloromethane, and other impurities subsequently eluted with neat dichloromethane. The $\text{CpFe}(\text{CO})(\text{P}(\text{OCH}_3)_3)(\text{C}(\text{O})\text{CH}_3)$ product was then eluted with a 20% acetonitrile/dichloromethane mixture and was isolated as an orange oil. This compound is quite air sensitive and must be stored in the dark under argon.

Apparatus and Procedures. The TRIR apparatus at Santa Barbara^{8,15} has a pump-probe configuration with an XeCl excimer (308 nm) laser excitation source and a tunable lead salt diode laser operating at a single, tunable IR frequency with a Hg:Cd:Te fast rise time detector to probe the sample. Response vs time traces were signal-averaged (>30 times) until a good s/n ratio was obtained. Data were converted to absorbance and analyzed according to exponential decays using Scopemate by UGI Scientific. TRIR spectra (e.g., Figure 1) were generated using Sigma Plot software to compile absorbance change (ΔAbs) vs time (t) traces recorded at different frequencies.

Low-temperature FTIR experiments were carried out using a PFD-FT12.5 Pourfill Dewar (R. G. Hansen and Associates) with a sample IR cell built to fit a Bio-Rad FTS-60 FTIR spectrometer. Solutions ($\sim 2 \times 10^{-3}$ M) for low-temperature IR experiments were prepared under argon and transferred to the deaerated cell using a gastight syringe. Initial FTIR spectra were measured at room temperature and again at low temperature by filling the Dewar with dry ice/acetone or LN_2 . The sample was irradiated with 5–10 excimer laser pulses ($\lambda_{\text{irr}} = 308$ nm), and spectra were collected to monitor formation and loss of intermediates and formation of products.

Hydrostatic pressure effects on quantum yields were investigated at Erlangen-Nürnberg on apparatus described elsewhere.¹⁶ The photolysis source was 313-nm light from a 200 W high-pressure, short-arc, mercury lamp. The sample solutions were prepared and transferred to a Le Noble pillbox cell¹⁷ in an inert-atmosphere box. The pillbox cell was mounted in the high-pressure cell housing, where the samples were

thermostated to 25.0 °C and stirred continuously during photolysis with a 2 mm Teflon-coated magnetic stir bar. In this configuration, photolyses were carried out at ambient pressure (0.1 MPa) and at applied pressures (P) of 50, 100, and 150 MPa. Light intensity was measured by a calibrated photodiode.

For experiments using UV-vis spectra to monitor solution changes, initial concentrations corresponded to an absorbance of $\sim 1.2 \text{ cm}^{-1}$, i.e., $[\mathbf{A}]_0 = 2.5 \times 10^{-4}$ M and $[\mathbf{A}_{\text{ind}}]_0 = 1.6 \times 10^{-4}$ M. Irradiation times under applied P were limited to that necessary to give $\sim 15\%$ photoreaction (~ 60 s). After photolysis, samples were transferred to a 1.0-cm cuvette for spectral analysis. Experiments using FTIR techniques to monitor solution changes were carried out analogously, but higher concentrations ($\sim 2 \times 10^{-3}$ M) and longer irradiation times (10–50 min) were used. After photolysis, samples were transferred by syringe to a 0.5-mm IR cell for analysis. Care was taken to minimize exposure of solutions to extraneous light during all experiments.

Treatment of Data from Pressure Experiments. The quantum yield (Φ_{I}) for formation of product \mathbf{P}_i from a photochemically generated intermediate \mathbf{I} is defined by

$$\Phi_{\text{I}} = \Phi_{\text{I}} \left(\frac{k_{\text{i}}}{\sum_j k_j} \right) \quad (2)$$

where Φ_{I} is the quantum yield for formation of \mathbf{I} , k_{i} is the rate constant for formation of \mathbf{P}_i from \mathbf{I} , and the summation includes all competitive processes by which \mathbf{I} is depleted. The partitioning between two competing reactions from \mathbf{I} equals the ratio of quantum yields, thus for Scheme 1

$$\frac{\Phi_{\text{L}}}{\Phi_{\text{m}}} = \frac{k_{\text{L}}[\text{L}]}{k_{\text{m}}} \quad (3)$$

Since the activation volume ($\Delta V_{\text{i}}^{\ddagger}$) for a pathway with the rate constant k_{i} is defined as¹⁸

$$\Delta V_{\text{i}}^{\ddagger} = -RT \left(\frac{\partial \ln k_{\text{i}}}{\partial P} \right)_T \quad (4)$$

the difference in the activation volumes for methyl migration and ligand substitution rates of \mathbf{I} can be calculated from pressure-induced changes in the quantum yield ratio according to

$$\Delta V_{\text{L}}^{\ddagger} - \Delta V_{\text{m}}^{\ddagger} = -RT \left(\frac{\partial \ln \left(\frac{\Phi_{\text{L}}}{\Phi_{\text{m}}} \right)}{\partial P} \right)_T + \left(\frac{\partial \ln [\text{L}]}{\partial P} \right)_T \quad (5)$$

The quantum yield ratio was determined from the changes in absorbances characteristic of the two products (i.e., $\Phi_{\text{L}}/\Phi_{\text{m}} = \Delta\text{Abs}_{\text{L}}/\Delta\text{Abs}_{\text{m}}$), and the latter term describes the effect of isothermal solvent compressibility on $[\text{L}]$ and may be estimated as $+3.0 \text{ cm}^3 \text{ mol}^{-1}$ based on the compressibility of heptane.¹⁹

Results

Time-Resolved Infrared Transient Spectra. Table 1 reports the ν_{CO} frequencies for the bands for the parent acetyl complex \mathbf{A} and for the photochemically generated intermediate \mathbf{I} determined from TRIR and low-temper-

(15) (a) DiBenedetto, J. A.; Ryba, D. W.; Ford, P. C. *Inorg. Chem.* **1989**, *28*, 3503–3507. (b) Ford, P. C.; DiBenedetto, J. A.; Ryba, D. W.; Belt, S. T. *SPIE Proceedings* **1636**, 1992, pp 9–16.

(16) Skibsted, L. H.; Weber, W.; van Eldik, R.; Kelm, H.; Ford, P. C. *Inorg. Chem.* **1983**, *22*, 541.

(17) Le Noble, W. J.; Schlott, R. *Rev. Sci. Instrum.* **1976**, *47*, 770.

(18) (a) van Eldik, R.; Asano, T.; Le Noble, W. J. *Chem. Rev.* **1989**, *89*, 549–688. (b) Ford, P. C. In *Inorganic High-Pressure Chemistry, Kinetics and Mechanisms*; van Eldik, R., Ed.; Elsevier: Amsterdam, 1986; Chapter 6, pp 295–338.

(19) (a) the compressibility of heptane is 13.4% per 100 MPa at 20 °C.^{21b} (b) Isaacs, N. S. *Liquid-Phase High-Pressure Photochemistry*; John Wiley & Sons: New York, 1981; p 66.

Table 1. Infrared Spectroscopic Data for the Parent Acetyl Complexes A and A_{ind} and for the Photogenerated Transient Species I and I_{ind}

A. Cyclopentadienyl Complexes				
solvent	$\nu_{\text{CO}}(\mathbf{A})$, cm^{-1}	$\nu_{\text{CO}}(\mathbf{I})$, cm^{-1}	method ^a	ref
PFMC	2025, 1969, 1676	1959	TRIR	<i>b</i>
cyclohexane	2018, 1963, 1669	1949	TRIR	2
isooctane	2018, 1962, 1670	1949	TRIR	2
hexane	2020, 1965, 1670	1949	TRIR	2
MCH ^c	2023/2018, 1968/1962, 1670/1627	1933, 1585	FTIR	<i>b</i>
CH ₂ Cl ₂	2020, 1961, 1620/1598	1940	TRIR	<i>b</i>
DCE ^d	2019, 1959, 1650/1609	1935	TRIR	<i>b</i>
2,5-Me ₂ THF	2012, 1956, 1655	1922	FTIR	<i>b</i>
2-MeTHF	2015, 1956, 1658	1920	TRIR	<i>b</i>
THF	2015, 1955, 1658	1921	TRIR	2
THF	2013, 1958, 1656	1917, ~1610	FTIR	<i>b</i>
acetonitrile	2018, 1958, 1650	1926	TRIR	2

B. Indenyl Complexes				
solvent	$\nu_{\text{CO}}(\mathbf{A}_{\text{ind}})$, cm^{-1}	$\nu_{\text{CO}}(\mathbf{I}_{\text{ind}})$, cm^{-1}	method	ref
cyclohexane	2016, 1961, 1671	1950	TRIR	<i>b</i>
THF	2013, 1954, 1660	1919	TRIR	<i>b</i>

^a TRIR experiments at 298 K, FTIR experiments at 195 K.

^b This work. ^c Methylcyclohexane. ^d 1,2-Dichloroethane.

ature FTIR spectra. The room-temperature FTIR spectrum of **A** shows only a modest solvent dependence; analogous ν_{CO} bands vary by less than 10 cm^{-1} in such disparate solvents as perfluoro(methylcyclohexane) (PFMC) and acetonitrile. In contrast, the TRIR spectra of **I** displayed a more notable trend. For each solvent, a single terminal CO stretching band was seen in the region and there was a general shift of ν_{CO} to lower frequency following (roughly) the increasing donor strength of the solvent: PFMC > cyclohexane > CH₂-Cl₂ > DCE > acetonitrile > MeTHF \approx THF,²⁰ consistent with the representation of **I** as the solvento species **S**. The acyl ν_{CO} band expected for **I** was generally not observable in the TRIR spectra, owing to its lower intensity and to interference from solvent absorbances. The positions of the ν_{CO} bands of the intermediate (**I_{ind}**) formed when the indenyl complex **A_{ind}** was photolyzed in cyclohexane (Figure 2) or THF proved to be very similar to those seen for the Cp analog in the respective solvents (Table 1).

Low-Temperature FTIR Spectra. The intermediate **I** could also be observed by FTIR methods when it was generated photochemically in 195 K solutions of methylcyclohexane, THF, or 2,5-Me₂THF (Table 1). (The poor solubility of **A** in PFMC prevented use of this medium at low *T*.) In agreement with previous work by Rest et al.,²¹ the FTIR spectrum of **A** in 195 K methylcyclohexane solution displays a split acyl ν_{CO} absorbance band, presumably due to different confor-

(20) The TRIR spectrum of intermediate **I** generated by flash photolysis of **A** in 2,2,5,5-tetramethyltetrahydrofuran (Me₄THF) (Aldrich) was also recorded. The single carbonyl stretching band showed a relatively low ν_{CO} value (1921 cm^{-1}), comparable to that seen in THF and 28 cm^{-1} lower than that seen in cyclohexane, although there was little difference in the ν_{CO} bands of **A** in this solvent (2017, 1962, 1669 cm^{-1}) and in cyclohexane (Table 1). This is surprising since the sterically crowded Me₄THF would be expected to be a less effective donor than THF. However, in this case, one must be concerned about possible coordination of isomeric impurities since the Me₄THF contained a small amount (~3%) of an isomeric component detectable by GC but not removed by distillation using a spinning band column. Such isomers may be better ligands.

(21) Hitam, R. B.; Narayanaswamy, R.; Rest, A. J. *J. Chem. Soc., Dalton Trans.* **1983**, 615.

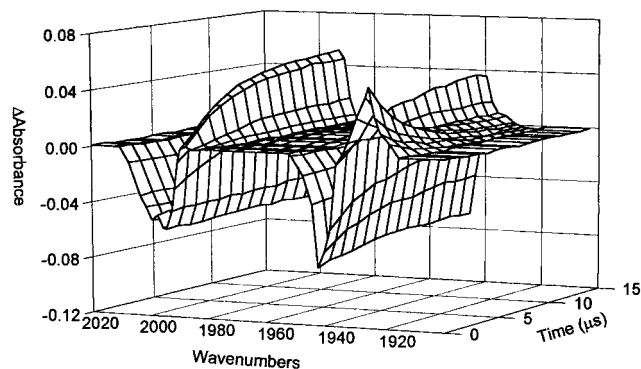


Figure 2. Temporal absorbance changes following 308-nm laser flash photolysis of a cyclohexane solution of **A_{ind}** (under argon at 295 K).

mations of the acyl group. Photolysis of this solution resulted in formation of a species with one terminal ν_{CO} at 1933 cm^{-1} and a weak acyl ν_{CO} absorbance at 1585 cm^{-1} . "Prompt" formation of **M** in a ratio of approximately 4:1 **I**:**M** was also seen, similar to observations in the low-temperature photolysis of Mn(CO)₅-(C(O)CH₃).⁸ These data compare to a preliminary study in 193 K liquid xenon, where 308 nm photolysis of **A** led to a transient species exhibiting ν_{CO} bands at 1938 and 1582 cm^{-1} , although in that case there was no significant formation of **M**.⁶ The ν_{CO} for **I** formed in 195 K THF and in 2,5-Me₂THF appeared at 1917 cm^{-1} and at 1922 cm^{-1} , respectively. These are lower frequencies than those found in the hydrocarbon MCH in the same manner as the room-temperature TRIR data. No prompt formation of **M** was observed in these two solvents.

Continuous Photolysis of A_{ind}. Photolysis (313 nm) of **A_{ind}** led to clean formation of **M_{ind}** in deaerated solutions of cyclohexane, heptane, and THF, as characterized by FTIR and UV-vis detection. The quantum efficiency of this process was found to be 0.34 (± 0.03), independent of solvent and of P_{CO} up to 1 atm. These results are analogous to those observed for photolysis of **A**, although the latter quantum yield (0.63)⁶ was about twice as large.

Reaction Dynamics of I and I_{ind}. The TRIR technique also provides rate data for reactions of the intermediates, i.e., intramolecular rearrangement to the methyl complexes (k_m) and reaction with ligands to give the substituted acetyl complexes ($k_L[\text{L}]$) (Scheme 1). The kinetics of such decays were, thus, probed for the intermediates resulting from flash photolysis of the cyclopentadienyliron complex **A** in various solvents and for the indenyl complex **A_{ind}** in cyclohexane. In each case, recombination of the intermediates with CO (up to 1 atm) was not competitive with the intramolecular rearrangement described by k_m , so only upper limits for k_{CO} ($\sim 6 \times 10^5$ and $\sim 3 \times 10^6 \text{ M}^{-1} \text{ s}^{-1}$, respectively) could be estimated for the two systems in cyclohexane ($[\text{CO}] = 0.0092 \text{ M atm}^{-1}$ at 25 °C).²² According to Scheme 1, it follows that $k_{\text{obs}} = k_m + k_L[\text{L}]$, and experiments collecting k_{obs} values as a function of $[\text{L}]$ should give a linear plot of k_{obs} vs $[\text{L}]$ with a slope of k_L and a *y*-intercept of k_m . Figure 3 is a such a plot for the photolysis of **A** in 295 K cyclohexane with $\text{L} = \text{P}(\text{OCH}_3)_3$. This gives $k_L = 3.6 \times 10^6 \text{ M}^{-1} \text{ s}^{-1}$ and $k_m = 5.9 \times 10^4$

(22) *IUPAC Solubility Data Series: Carbon Monoxide*, v. 43; Cargill, R. W., Ed.; Pergamon Press: New York, 1990.

Table 2. Rate Constants of the Intermediate CpFe(CO)(C(O)CH₃) (I) and (Ind)Fe(CO)(C(O)CH₃) (I_{ind}) at 295 K in Various Solvents^a

solvent	L	CpFe(CO)(C(O)CH ₃)		(Ind)Fe(CO)(C(O)CH ₃)	
		k_m (s ⁻¹)	k_L (M ⁻¹ s ⁻¹)	k_m (s ⁻¹)	k_L (M ⁻¹ s ⁻¹)
PFMC	P(OCH ₃) ₃	9.4×10^4	1.4×10^7		
cyclohexane	CO	5.7×10^{4b}	$<6 \times 10^{5b}$	2.8×10^5	$<3 \times 10^6$
cyclohexane	PPh ₃	5.6×10^{4b}	2.4×10^{6b}	2.8×10^5	1.2×10^7
cyclohexane	P(OCH ₃) ₃	5.9×10^4	3.6×10^6	2.8×10^5	2.1×10^7
CH ₂ Cl ₂	P(OCH ₃) ₃	1.4×10^5	4.3×10^5		
DCE ^c	P(OCH ₃) ₃	1.5×10^5	3×10^5		
2-Me THF	P(OCH ₃) ₃	3.9×10^4	2.5×10^5		
THF	P(OCH ₃) ₃	5.6×10^3	2.6×10^4		
acetonitrile	P(OCH ₃) ₃	$<1.0^b$	$<10^2$		

^a The reproducibilities of the rate constants reported are estimated as better than $\pm 10\%$. ^b Reference 6. ^c 1,2-Dichloroethane.

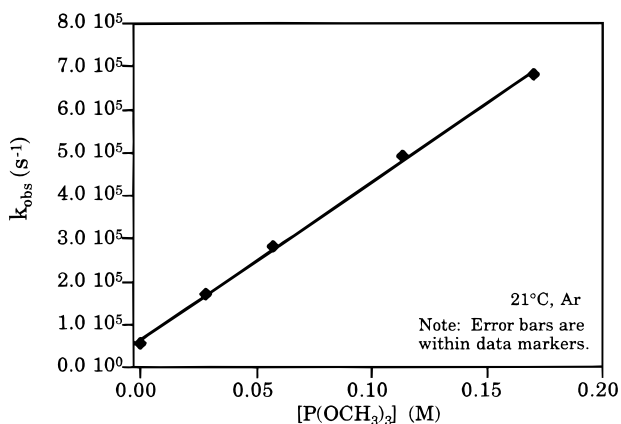


Figure 3. The observed rate constant for the disappearance of I measured by TRIR spectral techniques and plotted vs [P(OCH₃)₃] (cyclohexane solution under argon at 294 K).

Table 3. Comparison of Frequency Shifts (FS)^a Drawn from TRIR Spectra of I and the Rate Constants for Methyl Migration k_m and for Trapping by P(OCH₃)₃ k_L (295 K) in Various Solvents with Bond Energies (BE) for the Metal–Solvent Interaction for Chromium Pentacarbonyl (CO)₅Cr–Sol

solvent	FS ^a (cm ⁻¹)	k_m (s ⁻¹)	k_L (M ⁻¹ s ⁻¹)	BE (kcal/mol)
PFMC	38	9.4×10^4	1.4×10^7	$\leq 8^b$
isooctane ^c	41	4×10^4		
cyclohexane	42	5.7×10^4	3.6×10^6	12.6^d
hexane ^c	44	4×10^4		
CH ₂ Cl ₂	51	1.4×10^5	4.3×10^5	
DCE	54	1.5×10^5	3×10^5	15.6^d
MeTHF	69	3.9×10^4	2.5×10^5	21^d
THF	64	5.6×10^3	2.6×10^4	22.2^e
acetonitrile	62	<1.0	$<10^2$	28.0^e

^a See text (eq 8), fractional values rounded off. ^b Estimated from the value reported for C₆F₆ (ref 32c). ^c Reference 6. ^d Reference 32d. ^e Estimated, given values for THF (22.2 kcal/mol) and 2,5-dimethyl THF (20.6 kcal/mol) as given by ref 32a.

s⁻¹ in this medium, the latter value being very close to the k_m (5.7×10^4 s⁻¹) determined directly in the absence of added L.⁶

Table 3 summarizes k_m and k_L values determined for I in various solvents. From these data, it can be noted that k_L decreases in a trend (PFMC > cyclohexane > CH₂Cl₂ \approx DCE \approx 2-MeTHF > THF \gg acetonitrile) roughly parallel to the increasing donor ability of the solvent. In acetonitrile, the intermediate is so stable that its lifetime could not be measured on the TRIR apparatus. Rate constants k_m for methyl migration of I demonstrate a different order (DCE \approx CH₂Cl₂ >

PFMC > cyclohexane > isooctane \approx hexanes \approx MeTHF > THF \gg acetonitrile) but again are smaller in THF and (especially) acetonitrile than in the other solvents.²³

The k_m and k_L values determined similarly from linear k_{obs} vs [L] plots for I_{ind} in cyclohexane are also listed in Table 3. The k_m directly determined from kinetic traces in the absence of added ligand, 2.8×10^5 s⁻¹ in cyclohexane, had the same value as the intercepts of the k_{obs} vs [L] plots. For I_{ind} in this solvent, the k_m and the k_L values for L = PPh₃ and P(OMe)₃ were each ~ 5 times larger than the analogous rate constants for the Cp analogue I.

The reactions of the intermediate (I_{d3}) formed by flash photolysis of the trideuteriomethyl analogue CpFe(CO)₂(C(O)CD₃) (A_{d3}) were also examined by TRIR spectroscopy in order to probe isotope effects on methyl migration. In cyclohexane, the single ν_{CO} of I_{d3} occurs at 1950 cm⁻¹ and this disappears concomitant with the growth of bands for CpFe(CO)₂CD₃ (M_{d3}) at 2012 and 1963 cm⁻¹ (Figure 1). To ensure consistency, the k_m values for I and I_{d3} were measured under closely analogous conditions on the same day with the result $k_m^h/k_m^d = 1.1 \pm 0.1$. Attempts to detect C–D stretching frequencies in the TRIR spectra were unsuccessful.

Pressure Effects on Photoreactions. A previous study from these laboratories¹⁰ used rates of optical absorbance changes resulting from photolysis to evaluate the effects of applied hydrostatic pressure (P) on the competing reactions of I shown in Scheme 1. That study reported that the difference between the activation volumes of the k_L and k_m pathways ($\Delta\Delta V^\ddagger = \Delta V_L^\ddagger - \Delta V_m^\ddagger$) had a very large negative value. Subsequently, our attempts to repeat these experiments led to the conclusion that $\Delta\Delta V^\ddagger$ determined in this manner is extremely sensitive to small errors in extinction coefficient calculations since the absorption spectra of reactants and all products overlap. As a consequence, an apparent error of unknown origin in the experimental data, magnified by the method used to analyze that data, led to a serious exaggeration of the activation volume differences. Because of this problem, the work described here is a reevaluation of $\Delta\Delta V^\ddagger$ for the photochemical pathways of A using the far more selective FTIR spectral detection method, which is not subject

(23) Again, the somewhat questionable solvent²⁰ Me₄THF gave unexpected behavior. Although direct overlap of the intermediate and product absorbance peaks prevented accurate determination of k_L , the value determined for k_m (3×10^5 s⁻¹) was surprisingly large, suggesting that if indeed Me₄THF (or one of its isomers) is coordinated to the metal center, its lability is sufficiently large to favor the migration step.

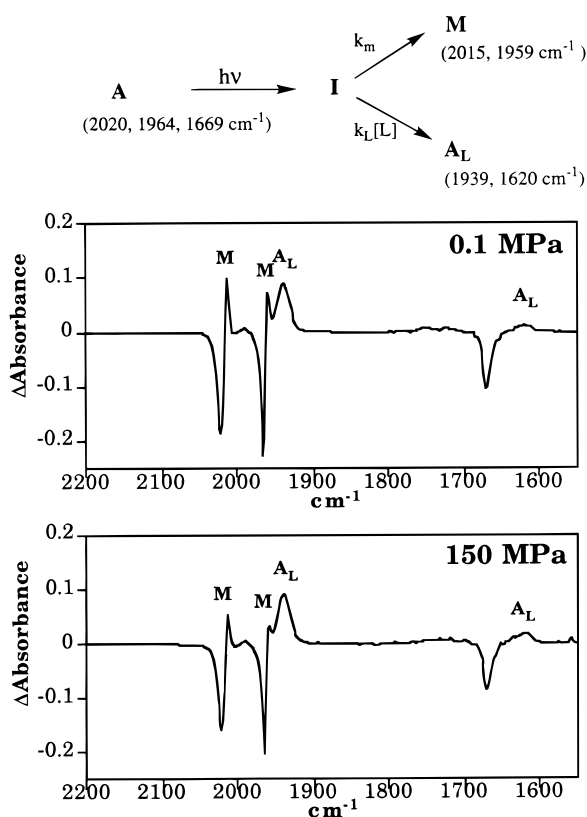


Figure 4. (a) Difference spectra from 313-nm photolysis of $\text{CpFe}(\text{CO})_2(\text{C}(\text{O})\text{CH}_3)$ at 0.1 MPa (ambient pressure) (upper figure). (b) Difference spectra from 313-nm photolysis of $\text{CpFe}(\text{CO})_2(\text{C}(\text{O})\text{CH}_3)$ at 150 MPa. Both experiments were carried out in identical heptane solutions in the presence of 0.02 M $\text{P}(\text{OCH}_3)_3$ (Ar, 298 K). **M** = $\text{CpFe}(\text{CO})_2\text{C}(\text{O})\text{CH}_3$; **A_L** = $\text{CpFe}(\text{CO})(\text{P}(\text{OCH}_3)_3)(\text{C}(\text{O})\text{CH}_3)$.

to similar error. Ratios of the photoproducts **M** and **A_L** formed under various pressures were determined, and eq 5 was used to calculate $\Delta V_{\text{L}}^{\ddagger} - \Delta V_{\text{m}}^{\ddagger}$.

The FTIR experiments are illustrated in Figure 4. Under ambient pressure ($P = 0.1$ MPa), photolysis of a heptane solution of **A** plus 0.02 M $\text{P}(\text{OCH}_3)_3$ led to formation of **M** and **A_L** in similar amounts according to the FTIR difference spectrum (Figure 4a), as expected from the rate constants. Under 150 MPa pressure, photolysis for the same time period resulted in a different partitioning of the products; formation of **M** was suppressed relative to **A_L** (Figure 4b). To analyze the relative concentrations of the photoproducts quantitatively, a subtraction factor which deleted the absorbances due to the residual starting complex was used to generate product spectra resulting from photolysis at 0.1 and 150 MPa. These data indicated that the $\Phi_{\text{L}}/\Phi_{\text{m}}$ quantum yield ratio increased from 1.0 at $P = 0.1$ MPa to 1.6 at 150 MPa.²⁴ Use of eq 5, which also corrects for the increased [L] resulting from solution compressibility,¹⁹ gave a $\Delta V_{\text{L}}^{\ddagger} - \Delta V_{\text{m}}^{\ddagger}$ value of -5 ± 1 $\text{cm}^3 \text{mol}^{-1}$ for the photolysis of **A**.²⁵

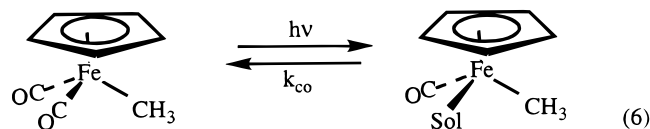
Analogous pressure experiments were also carried out with the indenyl complex **A_{ind}** at 0.1 and 150 MPa. Again, the partitioning between the ligand substitution and methyl migration pathways of **I_{ind}** was affected by pressure with **A_{Lind}** being more favored with respect to

M_{ind} at the higher P . From these FTIR data, $\Delta \Delta V^{\ddagger} = \Delta V_{\text{L}}^{\ddagger} - \Delta V_{\text{m}}^{\ddagger} = -5 \pm 1$ $\text{cm}^3 \text{mol}^{-1}$ was calculated.²⁵

Discussion

As stated above, this work sought to examine ambiguities that arose from previous investigations of reactive intermediates formed by flash photolysis of $\text{CpFe}(\text{CO})_2(\text{C}(\text{O})\text{CH}_3)$.^{6,10} Key questions are posed and discussed below.

*What is the structure of the photochemically generated intermediate **I** in lesser donating solvents?* Analysis of this question will be based on transient infrared spectra and kinetics determined by TRIR (ambient temperature) and low-temperature FTIR experiments, since the status of the empty coordination site in the photolabile species $\text{CpFe}(\text{CO})(\text{C}(\text{O})\text{CH}_3)$ (**I**) will be linked to the electronic environment around the metal center. Previous results here showed that the terminal ν_{CO} frequencies for **I** exhibit a significant solvent dependence when spectra in alkanes were compared to those in THF and acetonitrile and led to the conclusion that **I** is the solvento species **S** in the latter solvents.⁶ The more weakly donating alkanes could also coordinate,^{26,27} so a solvento complex might also be reasonable in these media. Indeed, in a separate study of transients generated by CO photodissociation from the methyl complex **M** in cyclohexane and THF (eq 6),²⁸ the species formed were interpreted to be the solvento complexes $\text{CpFe}(\text{CO})(\text{Sol})\text{CH}_3$, based (in part) on ν_{CO} appearing 28 cm^{-1} lower frequency in THF than in cyclohexane and (in part) upon the significantly lower rates of the reverse reaction in THF.



However, the acetyl ligand provides alternative possibilities not available for the methyl complex, i.e., intramolecular stabilization through η^2 -acetyl coordination (**C**) or through agostic interaction with the C–H bonds of the methyl group (**B**). For example, investigations of photochemically generated $\text{Mn}(\text{CO})_4(\text{C}(\text{O})\text{CH}_3)$ in room-temperature solutions⁸ and $\text{Co}(\text{CO})_3(\text{C}(\text{O})\text{CH}_3)$ in an argon matrix²⁹ show convincing evidence of η^2 -acetyl intermediates in alkane solvents, and theoretical

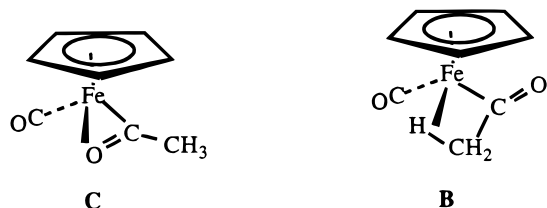
(25) The above FTIR spectral changes also gave estimates for the relative photoreactivities of **A** at different P . For example, under otherwise strictly analogous conditions, **A** underwent 24% depletion at ambient pressure but only 12% depletion at 150 MPa for the same irradiation time. From these differences, the apparent activation volume for the quantum yield of the decarbonylation of **A** ($\Delta V^{\ddagger}\Phi_{\text{d}}$) was estimated as $+11 \pm 2$ $\text{cm}^3 \text{mol}^{-1}$. When optical spectral changes were used instead, the estimated value of $\Delta V^{\ddagger}\Phi_{\text{d}}$ was $+9 \pm 2$ $\text{cm}^3 \text{mol}^{-1}$. Similarly, the loss of **A_{ind}** was evaluated quantitatively by monitoring absorbance changes of the acyl ν_{CO} absorbance at 1672 cm^{-1} , and from these data, $\Delta V^{\ddagger}\Phi_{\text{d}}$ for **A_{ind}** was estimated as $+13 \pm 2$ $\text{cm}^3 \text{mol}^{-1}$. However, at the higher pressure, the dimer $(\text{Ind})\text{Fe}(\text{CO})_2$ was also found to be a minor product, so homolytic cleavage of the Fe–acyl bond may be another pathway under these conditions.

(26) (a) Wieland, S.; Bal Reddy, K.; van Eldik, R. *Organometallics* **1990**, *9*, 1802–1806. (b) Zang, V.; Zhang, S.; Dobson, C. B.; Dobson, G. R.; van Eldik, R. *Organometallics* **1992**, *11*, 1154–1158. (c) Rossenaar, B. D.; van der Graaf, T.; van Eldik, R.; Langford, C. H.; Stufkens, D. J.; Vlcek, A., Jr. *Inorg. Chem.* **1994**, *33*, 2865–2873.

(27) (a) Creaven, B. S.; Dixon, A. J.; Kelly, J. M.; Long, C.; Poliakoff, M. *Organometallics* **1987**, *6*, 2600. (b) Wells, J. R.; Weitz, E. *J. Am. Chem. Soc.* **1992**, *114*, 2783–2787.

(28) McFarlane, K. L.; Ford, P. C. *Organometallics* **1998**, in press.

(24) On the basis of the extinction coefficient data: **A_L** ($\epsilon(1941 \text{ cm}^{-1}) = 3.9 \times 10^3 \text{ M}^{-1} \text{ cm}^{-1}$; **M** ($\epsilon(2014 \text{ cm}^{-1}) = 7.1 \times 10^3 \text{ M}^{-1} \text{ cm}^{-1}$ (heptane).



calculations on various structures of $\text{Mn}(\text{CO})_4(\text{C}(\text{O})\text{CH}_3)$ indicate that the η^2 -acyl mode is stable, more so than an agostic species.³⁰ On the other hand, NMR experiments on molybdenum acetyl complexes suggest the presence of agostic structures under static and dynamic conditions.³¹

Solvent-related shifts in ν_{CO} values of the monocarbonyl intermediate **I** are evident from inspection of Table 1. To separate the effects of specific interactions with the "vacant" coordination site from more global solvent perturbations on the spectra, a term "frequency shift" (FS) will be defined as the difference between the mean of the terminal ν_{CO} 's of **A** and the single ν_{CO} of **I** (i.e., $\text{FS} = \nu_{\text{CO}}(\text{ave})(\text{A}) - \nu_{\text{CO}}(\text{I})$). In each solvent, FS represents the expected shift of $\nu_{\text{CO}}(\text{I})$ to a lower frequency, since no candidate for coordination to the site vacated by CO photodissociation has π -acceptor properties comparable to that of CO itself. On the other hand, the relative magnitudes of FS should be reflective of the donor strength of that site's occupant.

While it would be desirable to compare such FS values to the metal-solvent bond energies (BE) in **S**, the data are not available for the CpFe-Sol system. Such BE values can be gathered³² for the solvento chromium pentacarbonyl prototype, i.e., $(\text{CO})_5\text{Cr-Sol}$. Table 3 compares FS values for **I** with BE values thus determined, and the general trend is clear that solvents giving the larger BE values also give the larger FS values. An exception is acetonitrile, which displays a smaller FS than does THF but shows a larger BE. This may be rationalized in terms of acetonitrile having some π -accepting ability which reduces the electron density at the metal.³³

The low temperature-experiments provide an interesting twist to this analysis. For each of the hydrocarbon solutions studied at room temperature, the FS value is nearly identical, i.e., $42 \pm 2 \text{ cm}^{-1}$, but in 195 K methylcyclohexane, FS is 60 cm^{-1} , larger by 18 cm^{-1} . In contrast, THF solutions at 295 and 195 K give the respective FS values 64 and 69 cm^{-1} , only a 5 cm^{-1} difference. Furthermore, the acyl ν_{CO} is shifted to much lower frequency upon conversion of **A** to **I** in 195 K

methylcyclohexane than in 195 K THF (Table 1). These observations suggest that **I** may have a different structure in 195 K MCH than it does in ambient temperature alkanes. Low $\nu_{\text{CO}}(\text{acyl})$ frequencies have been linked to η^2 -acyl coordination,³⁴ and coordination of an η^2 -acyl would explain the larger FS value in low-temperature MCH. Thus, in these weakly coordinating solvents, the equilibrium between the **S** and **C** configurations may be strongly temperature dependent with the η^2 -acyl form **C** being favored at the lower T . If so, similar coordination might be expected in the Xe(l) experiment noted above, since Xe binds less strongly to $\text{Cr}(\text{CO})_5$ (BE = 9.0 kcal/mol ²⁸) than do alkanes. Notably, the FTIR spectrum of **I** in 193 K Xe(l) displayed ν_{CO} bands at 1938 and 1581 cm^{-1} (FS = 55),^{6,35} very similar to the spectrum in 195 K methylcyclohexane glass.

The ligand substitution rate constants k_{L} for the photogenerated intermediate **I** also follow the general trend of the BE values for the $(\text{CO})_5\text{Cr-Sol}$ model, i.e., k_{L} values decrease with stronger M-Sol bonding. Although it is difficult to separate global solvent effects, these data suggest that Fe-Sol bond breaking is energetically important at the rate-limiting transition state of the reaction of L with **I**. However, rate differences alone are not sufficient to differentiate between a largely dissociative mechanism or an interchange pathway where bond formation to the metal center also plays a role. For both **I** and **I**_{ind} in cyclohexane solution, the k_{L} differences between L = PPh₃ and L = P(OCH₃)₃ are relatively small, implying that Fe-L bond formation is a relatively small contribution to the energy of the transition state. Such differences would be consistent with an interchange pathway where Fe-S bond breaking is concerted with Fe-L bond formation, consistent with the pressure effect described below. The low reactivity of CO with **I** ($k_{\text{CO}} < 6 \times 10^5 \text{ M}^{-1} \text{ s}^{-1}$ in cyclohexane) is interesting in the context of the much higher k_{CO} values (6×10^8 in cyclohexane and $3 \times 10^6 \text{ M}^{-1} \text{ s}^{-1}$ in THF) with the methyl analogue (eq 7).²⁸

Another issue should be considered. Even under 1 atm P_{CO} , trapping of **I** by CO is not competitive with the k_{m} pathway in any of these solvents. Thus, in PFMC, one can estimate that $k_{\text{CO}} \leq \sim 10^6 \text{ M}^{-1} \text{ s}^{-1}$ given the requirement $k_{\text{m}} \gg k_{\text{CO}}[\text{CO}]$; similarly, the upper limit for k_{CO} in cyclohexane was estimated to be $\sim 6 \times 10^5 \text{ M}^{-1} \text{ s}^{-1}$.⁶ For comparison, the rate constants for the reaction of $\text{Cr}(\text{CO})_5$ with CO in cyclohexane ($3 \times 10^6 \text{ M}^{-1} \text{ s}^{-1}$) is 3 orders of magnitude smaller than that in PFMC ($3 \times 10^9 \text{ M}^{-1} \text{ s}^{-1}$).³⁶ If a 1000-fold increase of k_{CO} occurred upon changing from alkane to perfluoroalkane solvent for **I** as well, the $k_{\text{CO}}[\text{CO}]$ pathway should compete with methyl migration in PFMC but does not. One could speculate that k_{CO} in cyclohexane is much smaller than the above upper limit, but considering the reactivity of **I** with PPh₃⁶ and P(OCH₃)₃ ($\sim 10^6 \text{ M}^{-1} \text{ s}^{-1}$), this seems unlikely. These comments lead to the question of whether **I** is the solvento complex **S** in PFMC. If not, the options would be agostic coordination as in **B** or η^2 -

(29) Sweany, R. L. *Organometallics* **1989**, *8*, 175-179.

(30) (a) Marynick, D. S. Personal communication to P. C. Ford. (b) Ziegler, T.; Verluise, L.; Tscinke, V. *J. Am. Chem. Soc.* **1986**, *108*, 612-617. (c) Rogers, J. R.; Kwon, O.; Marynick, D. S. *Organometallics* **1991**, *10*, 2816-2823.

(31) (a) Carmona, E.; Sánchez, L.; Marín, J. M.; Poveda, M. L.; Atwood, J. L.; Priester, R. D.; Rogers, R. D. *J. Am. Chem. Soc.* **1984**, *106*, 3214-3222. (b) Carmona, E.; Contreras, L.; Poveda, M. L.; Sánchez, L. *J. Am. Chem. Soc.* **1991**, *113*, 4322-4324.

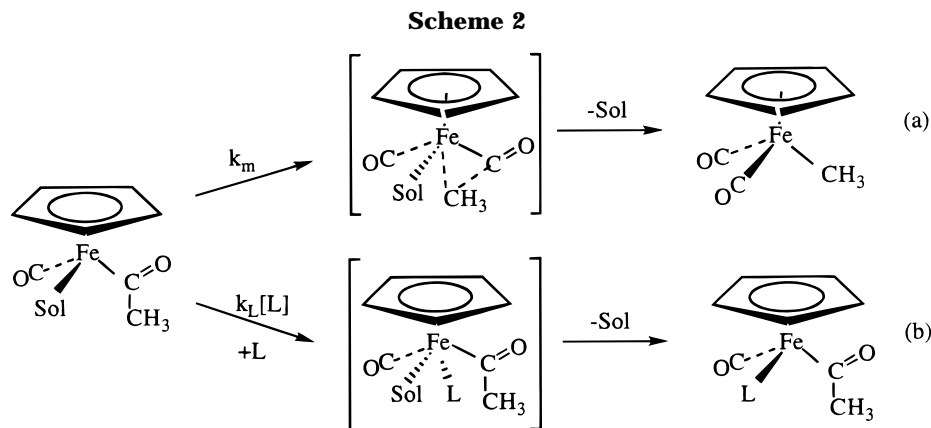
(32) (a) Yang, G. K.; Peters, K. S.; Vaida, V. *Chem. Phys. Lett.* **1986**, *125*, 3344. (b) Yang, G. K.; Vaida, V.; Peters, K. S. *Polyhedron* **1988**, *7*, 1619-1622. (c) Wells, J. R.; House, P. G.; Weitz, E. *J. Phys. Chem.* **1994**, *98*, 8384-8351. (d) Nayak, S. K.; Burkey, T. J. *Organometallics* **1991**, *10*, 3745-3750. (e) Burkey, T. J. In *Energetics of Organometallic Species*; Martinho Simões, J. A., Ed.; Kluwer Academic Publishers: Dordrecht, The Netherlands, 1992; pp 75-94. (f) Ishikawa, Y.; Brown, C. E.; Hackett, P. A.; Rayner, D. M. *Chem. Phys. Lett.* **1988**, *150*, 506.

(33) (a) Clarke, R. E.; Ford, P. C. *Inorg. Chem.* **1970**, *9*, 227. (b) Foust, R. D., Jr.; Ford, P. C. *J. Am. Chem. Soc.* **1972**, *94*, 6665.

(34) Durfee, L. D.; Rothwell, I. P. *Chem. Rev.* **1988**, *88*, 1059-1079.

(35) Ryba, D. W. Ph.D. Dissertation, University of California, 1991; Chapter 4.

(36) (a) Kelly, J. M.; Hermann, H.; von Gustorf, E. K. *J. Chem. Soc., Chem. Commun.* **1973**, 105-106. (b) Bonneau, R.; Kelly, J. M. *J. Am. Chem. Soc.* **1980**, *102*, 1220-1221.



acyl coordination as in **C**. Given that FS in PFMC is quite close to the FS values found in the various alkanes at room temperature, the former possibility appears the more attractive.

*Does ligand substitution on **I** involve a ring-slip mechanism?* The photochemical properties of the indenyl and Cp compounds **A_{ind}** and **A** are quite similar. Flash photolysis studies show that both form monocarbonyl intermediates, **I_{ind}** and **I**, respectively, which undergo competitive trapping by ligands **L** (k_L) and methyl migration (k_m) to the methyl analogues **M_{ind}** and **M**. The reactivity of **I_{ind}** is modestly greater than that of **I**, with k_m and k_L values each about 5-fold greater. These differences are much smaller than the rate enhancements used to argue for a ring-slippage mechanism involving formation of an η^3 transition state in the rate-limiting process. For example, the k_L for reaction of PPh₃ with CpRh(CO)₂ is 8 orders of magnitude smaller than for the reaction with the indenyl complex (Ind)Rh(CO)₂.³⁷ Such observations have been made in other η^5 complexes.³⁸ Since k_L and k_m of the photochemically generated intermediates both show only modest rate accelerations upon replacement of Cp by Ind, it may be argued that a ring-slippage intermediate does not play a major role in either the methyl-migration or ligand-substitution reactions of **I** (or **I_{ind}**).

How is the partitioning between the k_m and k_L pathways affected by pressure? The hydrostatic pressure experiments reported here demonstrate that the very large negative activation volume difference $\Delta V_L^\ddagger - \Delta V_m^\ddagger$ reported previously from these laboratories was incorrect in magnitude (too large) but not in sign.¹⁰ The earlier pressure results were, indeed, partially responsible for launching the present search for an indenyl effect, but this apparently resulted from experimental error exaggerated by the data analysis method (see Results section). The present data indicate that $\Delta\Delta V^\ddagger$ has a value of $-5 \text{ cm}^3 \text{ mol}^{-1}$ for both the Cp and indenyl compounds, i.e., the activation volume for the ligand substitution pathway on **I** (or **I_{ind}**) to give **A_L** (or **A_{Lind}**) is more negative than that for the competing methyl migration pathway of **I** (or **I_{ind}**) to give **M** (or **M_{ind}**). These $\Delta\Delta V^\ddagger$ values suggest transition states which are not dramatically different in character for these two pathways (and for the respective Cp and Ind compounds). This view is further substantiated by the

similar, but modest, rate accelerations experienced by both the k_m and k_L pathways upon substituting an indenyl ring for the cyclopentadienyl ring.

One possible scenario is illustrated by Scheme 2, where both pathways are concerted reactions of the solvento species. In this scenario, methyl migration occurs simultaneous with Fe–Sol bond cleavage while ligand substitution occurs through an interchange mechanism. In both cases, Fe–Sol bond breaking might be expected to be simultaneous with Fe–CH₃ or Fe–L bond formation, respectively. Since the ligand substitution rate is moderately sensitive to both the concentration and nature of L, Fe–L bond formation is energetically significant at the transition state of the k_L pathway. In such a scenario, this pathway should display a negative ΔV_L^\ddagger , although the magnitude would depend on the extent of bond formation to L relative to dissociation of the weaker Fe–Sol bond. It is clear that values of k_L for **I** are sensitive to the apparent M–Sol bond strengths but not to such an extent as suggesting a dissociative mechanism. The intramolecular k_m pathway is much less sensitive, so Fe–Sol bond breaking may be less developed at the transition state for methyl migration. In such a case, a ΔV_m^\ddagger near zero might be predicted, although the need for the acetyl group to adopt a configuration appropriate for methyl transfer might lead to a small negative value. In other words, it appears that the -5 cm^3 value for $\Delta\Delta V^\ddagger$ can be entirely attributed to ΔV_L^\ddagger ; indeed ΔV_L^\ddagger may be more negative than -5 cm^3 . In this context, the similarity in $\Delta\Delta V^\ddagger$ values for **I** and for **I_{ind}** argues that the substitution pathway for the latter does not have greater associative character in its transition state.

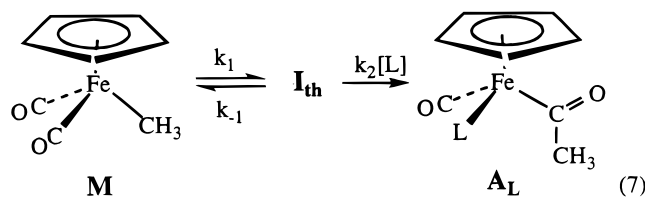
*What is the relationship between the intermediates **I** and **I_{ind}** and the mechanism for thermal migratory insertion?* Although qualitative studies of the carbonylations of **M** and **M_{ind}** are suggestive of an “indenyl effect” in the migratory insertion reactions of such complexes,³⁹ recent quantitative studies by Bassetti et al. regarding thermal reactions of different phosphines with these substrates to give the respective substituted acetyl complexes show little evidence supporting a ring-slip mechanism.⁴⁰ Under comparable conditions in THF solution, the reaction of PPh₃ is about an order of magnitude faster with **M_{ind}** than with **M** but it is notable that the effect was less than other system

(37) Rerek, M. E.; Ji, L.-N.; Basolo, F. *J. Chem. Soc., Chem. Commun.* **1983**, 1208–1209.

(38) Basolo, F. *N. J. Chem.* **1994**, *18*, 19–24.

(39) (a) Forschner, T. C.; Cutler, A. R. *Organometallics* **1985**, *4*, 1247–1257.

perturbations, e.g., replacement of $-\text{CH}_3$ with $-\text{CH}(\text{CH}_3)_2$ as the migrating group.^{40c} These authors noted that k_{obs} for the thermal reaction is phosphine concentration dependent but demonstrates saturation effects at higher $[\text{R}_3\text{P}]$. They interpreted this in terms of the formation of an outer-sphere complex between the metal alkyl (e.g., **M**) and the phosphine followed by a concerted step where L associates with the iron simultaneous with alkyl migration. The alternative of a slow, reversible migration step (k_1) to form an ("unsaturated" or solvento) intermediate coupled with competitive rapid reversal from intermediate to starting material (k_{-1}) and trapping with L ($k_2[\text{L}]$) (e.g., eq 7) could not be excluded for the reactions in THF,^{40c} although credible arguments based on k_{obs} values in toluene were presented in support of the preequilibrium mechanism.^{40b} For ex-



ample, in the latter solvent, electron-withdrawing substituents on aryl phosphines ($\text{P}(\text{Ar}-x)_3$) appear to favor the reaction, an observation consistent with the proposed outer-sphere complex having charge-transfer character. Nonetheless, THF solutions of **M** or **M_{ind}** with sufficient $[\text{L}]$ to give proportionally high concentrations of the outer-sphere complex⁴⁰ failed to give a spectroscopic signature consistent with such a species.

The present work addresses the kinetics behavior of the "unsaturated" transient **I** (or its solvento analog) which would have the same composition as **I_{th}** if the latter is formed by a unimolecular or solvent-assisted rearrangement and is not a concerted reaction of **M** with L. Despite their photochemical origin, transients such as **I** or **I_{ind}** are sufficiently long-lived that they are neither electronic nor vibronic excited states, so the rates of their competitive reactions should be identical those of the same species generated along a thermal reaction coordinate under identical conditions. Furthermore, according to the principle of microscopic reversibility, the properties of a rate-limiting transition state sampled by probing systematic effects on migration of the alkyl group from the acyl to the metal are relevant to the forward reaction, i.e., migration of the alkyl from the metal to a coordinated carbonyl. Whether the latter pathway is relevant to the overall mechanism of the thermal migratory insertion reaction is dependent on the relative ΔG^\ddagger values of competing pathways such as the proposed preequilibrium discussed above or a concerted attack of L without intermediates. In this context, analysis of the thermal kinetics in THF,^{40c} assuming the eq 7 mechanism, allows one to determine the ratio k_2/k_{-1} for purported trapping of **I_{th}** by L vs rapid reversal to **M**. This ratio should equal k_1/k_m (Scheme 1) if the same intermediates are involved and the conditions are the same. Owing to hardware

limitations, the photochemical experiment was not carried out at the higher temperatures necessary to measure the thermal kinetics, but since both k_2 and k_{-1} should have relatively low ΔH^\ddagger values, their ratio should not be strongly temperature dependent. Thus, for the reaction of **M** with PPh_3 , such analysis gives $k_2/k_{-1} = 2.8 \text{ M}^{-1}$ in 323 K THF; for comparison, the k_1/k_m ratio measured in 295 K THF by TRIR is 4.6 M^{-1} , comparable although not identical. This is consistent with, but certainly not proof of, mechanistic congruence. However, formation of the solvento form of **I** (i.e. **S**) along the thermal reaction coordinate would indeed be consistent with the long known role of donor solvents in assisting the reactions of **M** with phosphines to give **A_L**.^{4a}

Summary. The spectra and reaction dynamics of the "unsaturated" intermediate(s) **I** formed when the acetyl species **A** is subjected to flash photolysis in fluid solutions are best interpreted in terms of formation of the solvento complexes $\text{CpFe}(\text{CO})(\text{Sol})(\text{C}(\text{O})\text{CH}_3)$. Exceptions to this conclusion appear to be likely in the perfluorinated solvent PFMC and in low-temperature media such as in 195 K methylcyclohexane. A reexamination of the pressure effects on the partitioning between methyl migration and trapping by the ligand $\text{P}(\text{OCH}_3)_3$ demonstrated that, indeed, the latter pathway has a more negative volume of activation than the former, but the earlier report from these laboratories¹⁰ seriously overestimated this value. Last, the time-resolved spectral properties and dynamics of intermediates formed by flash photolysis of the indenyl complex **A_{ind}** are quite similar to those from the cyclopentadienyl analogue **A**, as are the respective pressure effects. These observations argue against a ring-slip mechanism having a significant influence on the pathways leading to the decay of the intermediates **I** and **I_{ind}** generated photochemically. The reactivity patterns noted for **I** are not inconsistent with those seen for potential intermediates formed along the reaction coordinate for the phosphine-promoted migratory insertion reaction of the alkyl species **M** to give the acyl complex **A_L**. However, the behavioral similarity of **I** and **I_{ind}** suggests that such intermediates may not lie along the reaction coordinate for direct carbonylation, since the qualitative data regarding the direct carbonylation of **M** and **M_{ind}** indicate the much greater reactivity of the latter.³⁹ The reason for this may lie in the low reactivity of **I** (and of **I_{ind}**) toward CO in competition with the reverse reaction (k_{-1} or k_m step) in any solvent considered here. An alternative pathway, perhaps involving an associative reaction of CO with **M** to give an η^3 Cp tricarbonyl intermediate, may be the lower energy mechanism.

Acknowledgment. Studies at UCSB have been sponsored by a grant to P.C.F. from the Division of Chemical Sciences, Office of Basic Energy Sciences, U.S. Department of Energy (Grant No. DE-FG03-85ER13317). Support for instrumentation development came from a U.S. Department of Energy University Research Instrumentation Grant (No. DE-FG05-91ER79039) and the U.S. National Science Foundation Instrumentation Grant (No. CHE-9413030). Studies at the University of Erlangen-Nürnberg were supported by a NATO Grant (No. 910187) to R.v.E. and P.C.F. We thank Dr. Ivan Lorkovic' for help in the synthesis of certain compounds.

(40) (a) Monti, D.; Bassetti, M. *J. Am. Chem. Soc.* **1993**, *115*, 4658–4664. (b) Bassetti, M.; Mannina, L.; Monti, D. *Organometallics* **1994**, *13*, 3293–3299. (c) Allevi, M.; Bassetti, M.; Lo, C.; Monti, D. *J. Chem. Soc., Dalton Trans.* **1996**, 3727–3531.